Supplementary information for: Hidden Markov models applied to LFPs from layer two and three of human cortex reveal highly stereotypical electrophysiological activity in epileptic seizures separated by hours

Joaquin Rapela Dmitrii Todorov

February 23, 2019

1 Introduction

In the main text of this article we presented evidence suggesting that seizures can be described as sequences of long-duration discrete states that are highly stereotypical across three seizures separated by more than one hour, in agreement with previous studies (Truccolo et al., 2011; Wagner et al., 2015) that analyzed seizures from the same microelectrode array recordings that we studied in the main text. Here we extend these previous studies, by showing that pre- and post-ictal periods from the three previous seizures can also be well characterized as sequences of long-duration discrete states that are highly stereotypical.

Sections 2.1 and 2.2 present the analysis of post- and pre-ictal seizure periods, Section 3 provides a brief discussion of this analysis and Appendix A gives interactive versions of Figures 1, 2 and 5 in the main text.

2 Results

2.1 Post-Ictal Periods

Figures 1a, b and c show the fractional occupancy in seizure blocks 1, 2, and 3, respectively. In each of the three seizures blocks we identified two states that were active (i.e., have fractional occupancy different from zero) mostly in post-ictal periods. In each of these three blocks, one state, labeled state D, had large fractional occupancy immediately after seizure termination, which decreased at later times. The fractional occupancy of the other state, labeled state E, was small immediately after seizure termination and increased subsequently. Thus, Figure 1 shows two post-ictal states with similar temporal activation's across three seizure blocks separated by more than one hour.

Figure 2 plots the power spectrum of states D and E in the three seizure blocks. We see that the power spectrums of the two states (cyan or magenta lines) are remarkably similar across blocks (panels a-c). Also, within each block the power spectrum of state E (cyan line) was larger than that of state D (magenta line) across all frequencies.

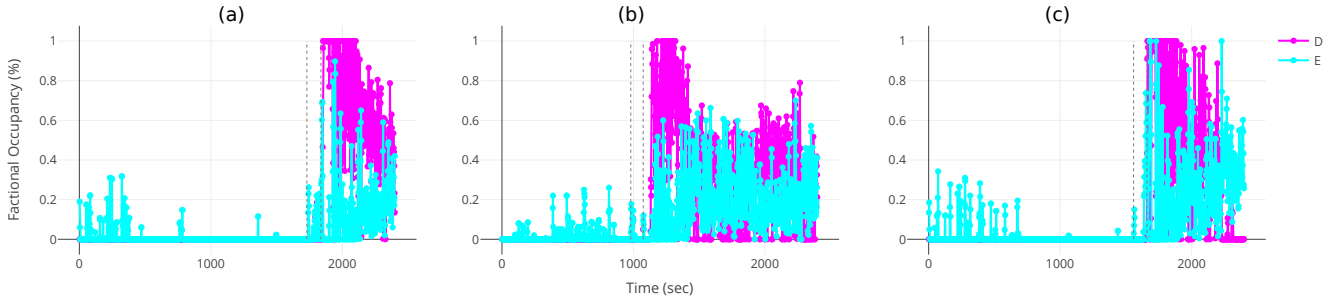

Figure 1: Fractional occupancies of post-ictal states for blocks one (a), two (b) and three (c). In each block, we call state D to the state whose fractional occupancy was large immediately after the seizure and decreases afterward. We call state E to the state whose fractional occupancy was small immediately after the seizure and increases afterward. The first and second dotted vertical lines indicate times of seizure initiation and termination, respectively. The activation timing of the two post-ictal states was remarkably similar across seizure blocks separated by more than one hour. Click on a panel to see its interactive version.

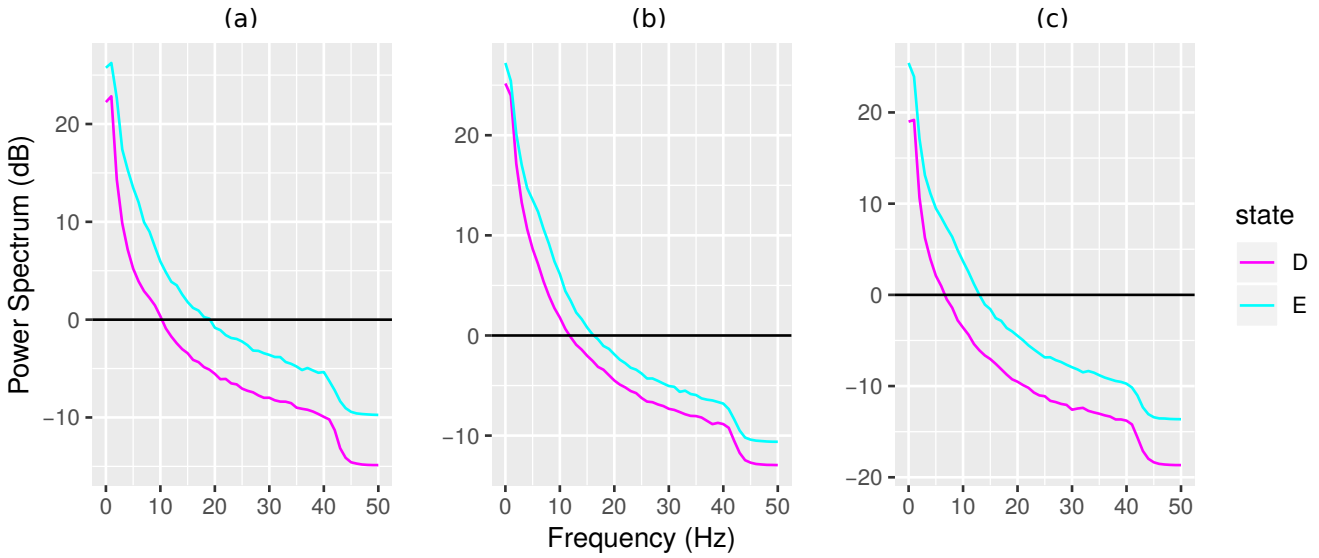

Figure 2: Power spectrum of post-ictal states in blocks one (a), two (b) and three (c). Across different blocks, the power spectrums of a state are very similar (e.g., the power spectrum of state D, magenta line, was very similar across blocks, panels a-c). Within any block, the power spectrum of state E was larger than that of state D, for all frequencies (i.e, the cyan curve was always larger than the magenta one in any panel a-c).

Figure 3 plots the autocorrelations of the the two post-ictal states. It shows that for any state (magenta or cyan curve) the autocorrelations are very similar across the three blocks (panels a-c) and that for any block the autocorrelation of state E (cyan curve) was smaller/larger than that of state D (magenta curve) for lags smaller/larger than 0.5 sec.

Figure 4 plots the coefficients and the mean and variance of the autoregressive models corresponding to the two post-ictal states (magenta and cyan curves) for the three seizure blocks (panels a-c). These coefficients are similar across the three blocks, with peak values around a delay 12 (120 ms). Within a block the coefficients of states D and E were also very similar, but the variance of the autoregressive model corresponding to state E was larger than that of state E (i.e., s2 was larger for the cyan caption than for the magenta caption).

2.2 Pre-Ictal Periods

Figure 5 plots the fractional occupancies of two states found to be active mostly during pre-ictal periods. We label state F (state G) to the state with larger (smaller) fractional occupancy in the pre-ictal period. At most pre-ictal times state F was more active (i.e., had larger fractional occupancy) than state G in seizure blocks one and three (panels a and c), and to a lesser degree in seizure block two (panel b).

Across blocks the power spectrums (Figure 6), autocorrelations (Figure 7) and coefficients, mean and variance of autoregressive models (Figure 8) of a state were very similar. Within a block the power spectrums (Figure 6), autocorrelations (Figure 7) and coefficients, mean and variance of autoregressive models (Figure 8) of state F (orange curve) and state G (violet curve) were different from each other. The similarity across blocks of power spectrums, autocorrelations and coefficients, mean and variances of autoregressive models was stronger between blocks one and three (panels a and c) than between any block and block two (between any panel and panel b).

3 Discussion

Using hidden-Markov models (HMMs) we have found discrete states in post- and pre-ictal periods with statistical properties (e.g., autocorrelation function, power spectrum, coefficients and variance of autoregressive models) that are consistent across seizure blocks separated by more than one hour. For post-ictal periods this consistency held across the three seizure blocks (Figure 2, 3, 4) and for pre-ictal periods this consistency was stronger between blocks one and three than between any block and block two (Figure 6, 7, 8).

With our high-density micro-electrode array recordings from cortical layers two and three of humans have shown that HMMs separate ictal, pre- and post-ictal local-field potentials into discrete states that are consistent across seizure blocks separated by more than one hour. That is, HMMs identify invariants in ictal, pre- and post-ictal LFPs extracted from high-resolution micro-electrode array recordings from cortical layers two and three of humans.

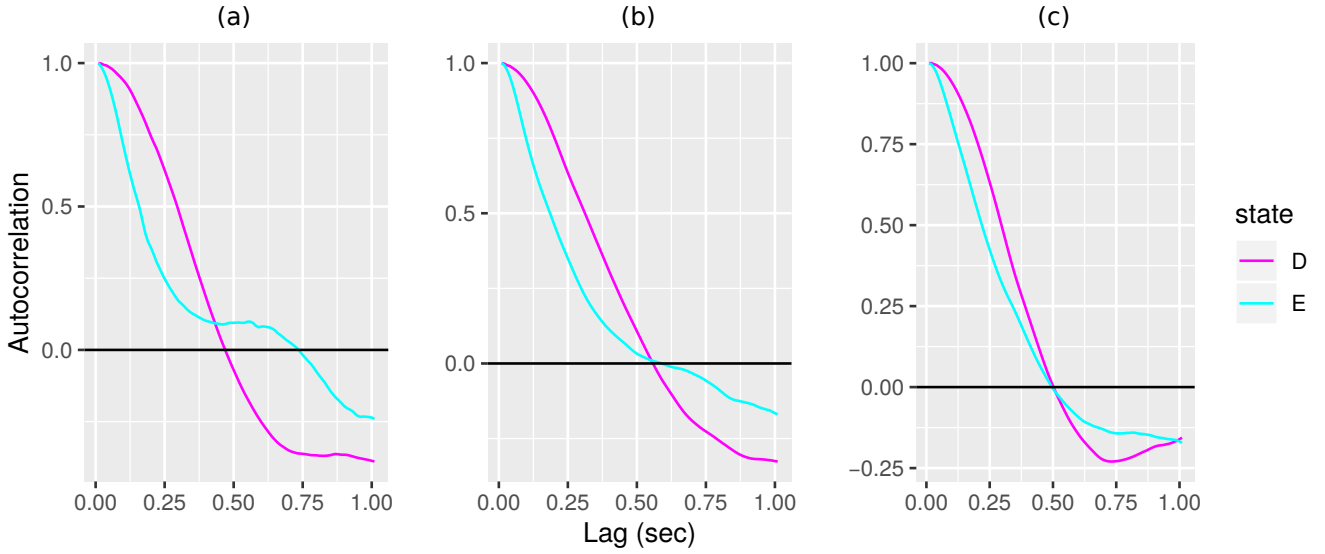

Figure 3: Autocorrelation of post-ictal states in blocks one (a), two (b) and three (c). The autocorrelations of both states are similar across different blocks (panels a-c) and within each block the autocorrelation of state D was different from that of state E.

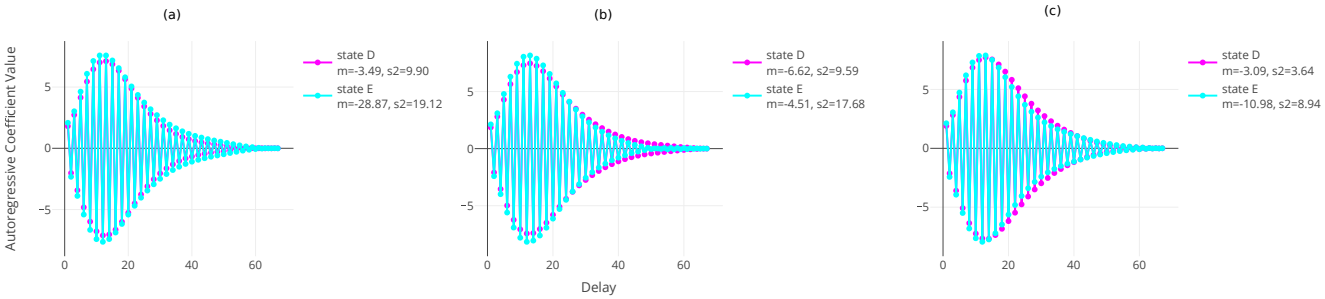

Figure 4: Coefficients, means and variances of autoregressive models for post-ictal states in blocks one (a), two (b) and three (c). Across seizure blocks (panels a-c), the coefficients of any state (cyan or magenta curves) where similar. Within each block the variance of the autoregressive model corresponding to state E (s2 in cyan caption) was larger than that corresponding to state D (s2 in magenta caption). Click on a panel to see its interactive version.

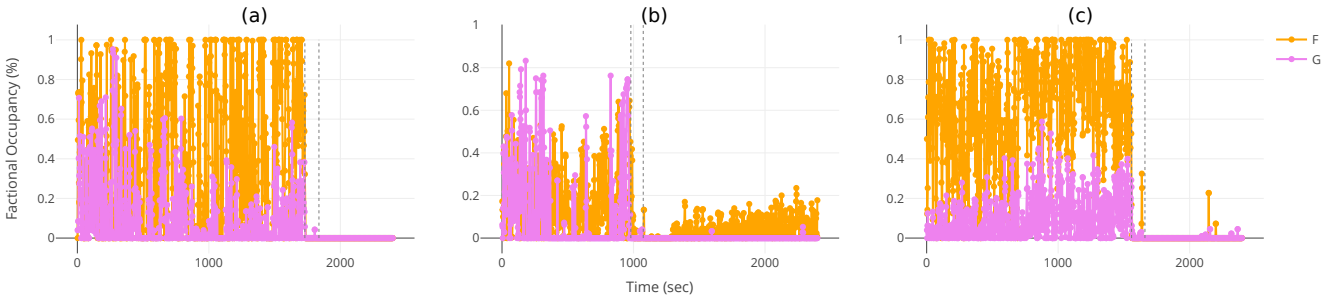

Figure 5: Fractional occupancies of pre-ictal states for blocks one (a), two (b) and three (c). In each block we call state F (G) to the state whose fractional occupancy was larger (smaller) in the pre-ictal period. At most pre-ictal times state F was more active (i.e., had larger fractional occupancy) than state G in seizure blocks one and three (panels a and c), and to a lesser degree in seizure block two (panel b). Click on a panel to see its interactive version.

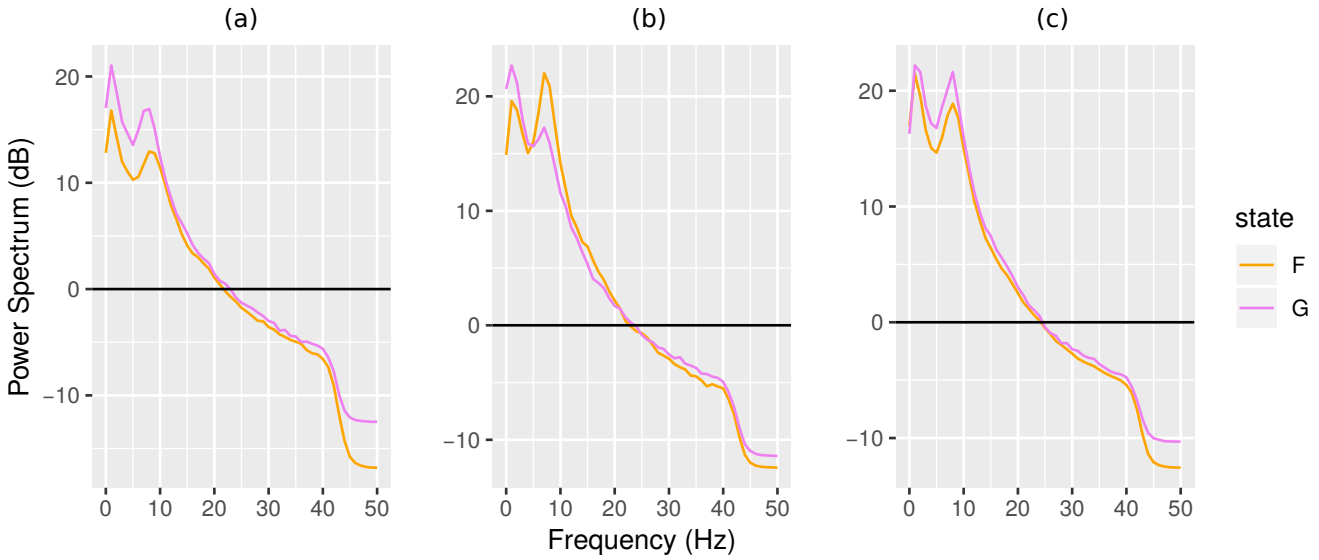

Figure 6: Power spectrum of pre-ictal states in blocks one (a), two (b) and three (c). Across blocks, the power spectrums of a given state were very similar. Within each block, the power spectrum of state G was larger than that of state F, for all frequencies. The consistency of power spectrums across blocks was stronger between blocks one and three, than between any block and block 2.

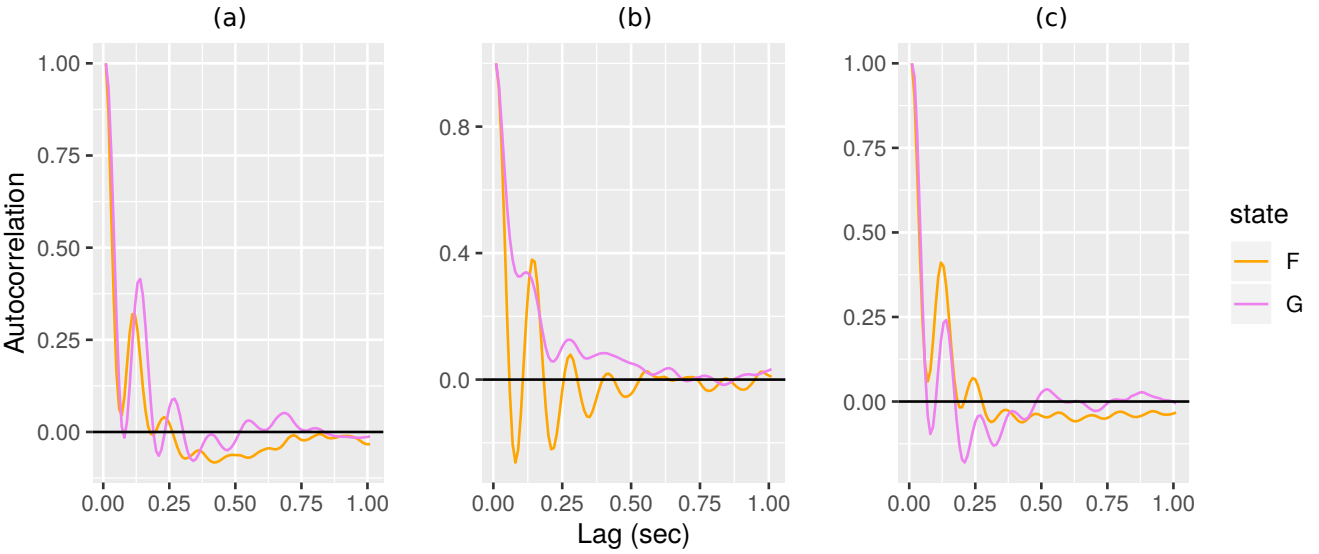

Figure 7: Autocorrelation of pre-ictal states in blocks one (a), two (b) and three (c). The autocorrelations of a given state were very similar across blocks and within one block the autocorrelations of the the two states were different (e.g., the orange curve was similar across panels a-c, and for panel a the orange and violet curves were different). These observations were stronger between blocks 1 and 3 (i.e., between panels a and c).

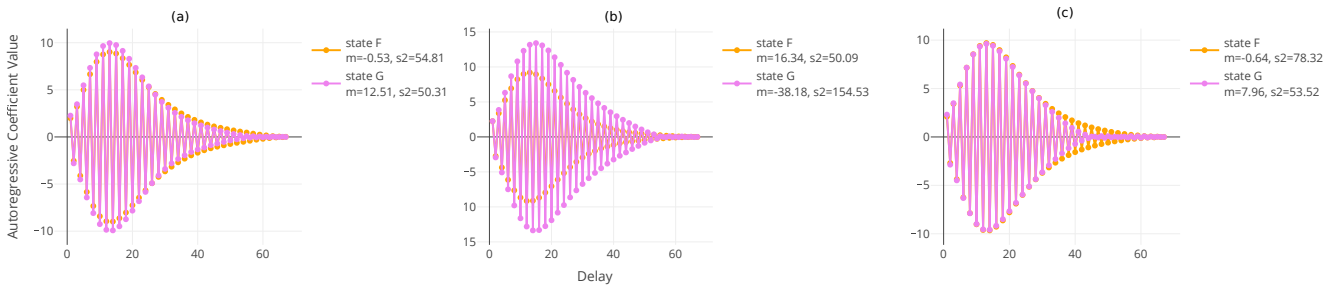

Figure 8: Coefficients, means and variances of autoregressive models for pre-ictal states in blocks one (a), two (b) and three (c). Across seizure blocks, the coefficients of any state were similar. Within a block, the mean (variable m in state legend) of the autoregressive model for state G was larger than that for state F. Also, within a block, the variance (variable $s2$ in state legend) of the autoregressive model for state G was smaller than that for state F. The previous observations hold fully for blocks one and three (panels a, c) and only partially for block two (panel b). Click on a panel to see its interactive version.

Appendix A Interactive version of figures in the main text

Figures 9, 10 and 11 are interactive versions of the main text Figures 1, 2 and 5, respectively.

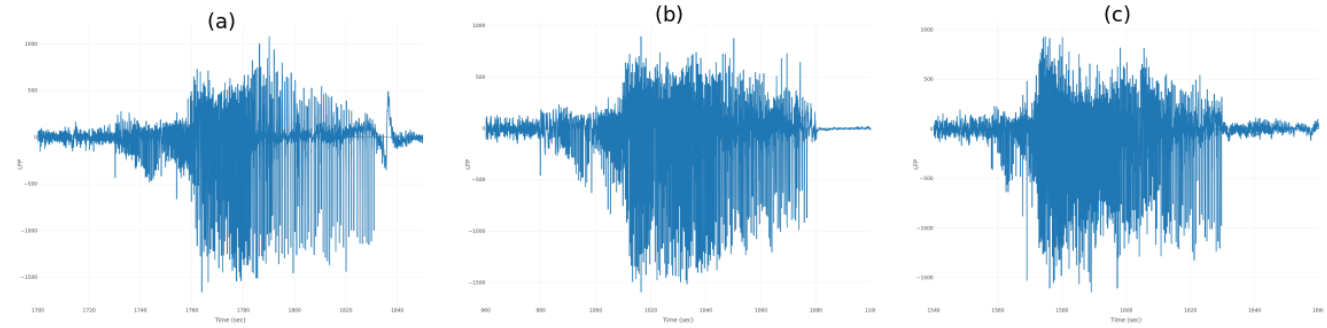

Figure 9: LFPs of spike-and-wave seizures in blocks one (a), two (b) and three (c). Click on a panel to see its interactive version.

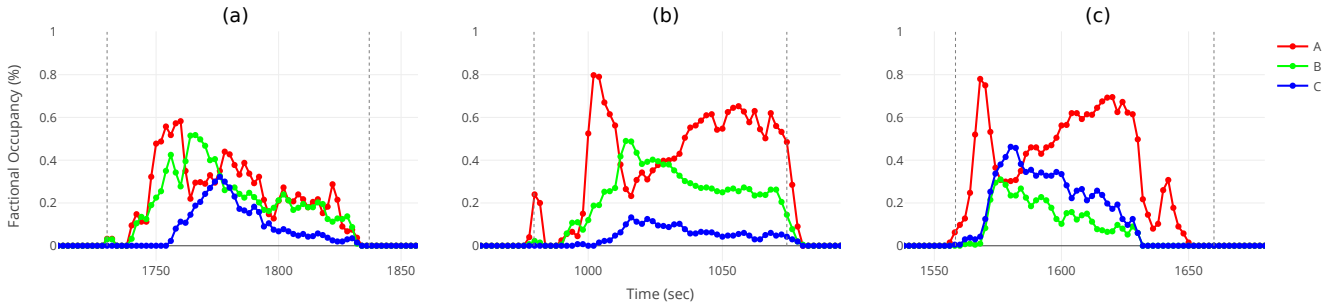

Figure 10: Fractional occupancies of ictal states for blocks one (a), two (b) and three (c). For any ictal state, the shapes of its fractional occupancy curves were similar across the three recording blocks. Click on a panel to see its interactive version.

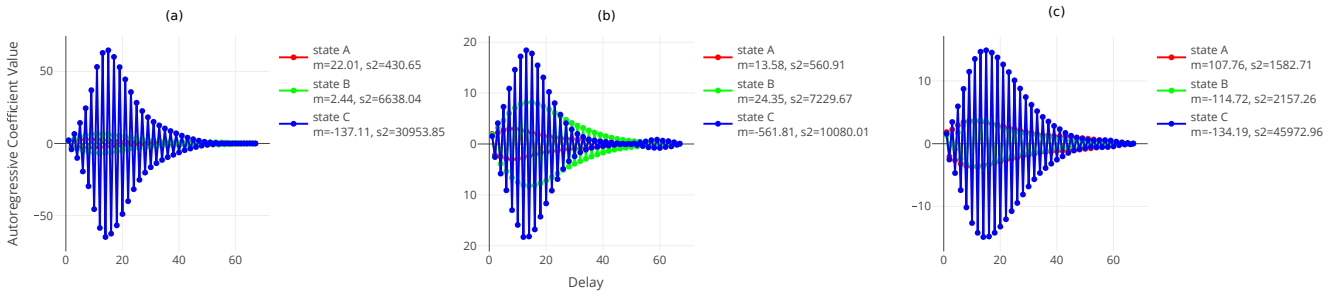

Figure 11: Coefficients, means and variances of autoregressive models for ictal states in blocks one (a), two (b) and three (c). Click on a panel to see its interactive version.

References

Truccolo, W., Donoghue, J. A., Hochberg, L. R., Eskandar, E. N., Madsen, J. R., Anderson, W. S., ... Cash, S. S. (2011). Single-neuron dynamics in human focal epilepsy. *Nature neuroscience*, *14*(5), 635.

Wagner, F. B., Eskandar, E. N., Cosgrove, G. R., Madsen, J. R., Blum, A. S., Potter, N. S., ... Truccolo, W. (2015). Microscale spatiotemporal dynamics during neocortical propagation of human focal seizures. *Neuroimage*, *122*, 114–130.